Korean J. of Chem. Eng., **14**(1), 8-14 (1997)

STRUCTURAL CHANGE OF POLYDOMAIN IN THE LIQUID CRYSTALLINE POLYMERS BY WEAK SHEAR FLOW

Kwang Man Kim, Tae Kyun Kim, Sanghyo Kim* and In Jae Chung†

Department of Chemical Engineering, Korea Advanced Institute of Science and Technology (KAIST), 373-1 Kusong, Yusong, Taejon 305-701, Korea

(Received 19 March 1996 • accepted 15 November 1996)

Abstract – Steady-state shear stress ($\bar{\tau}_{12}$) and first normal stress difference (N_1) of liquid crystalline polymers at low shear rates were examined by using a mesoscopic constitutive equation set including the idea of initial domain size. For the applicability to the weak shear flow at low shear rates, a Hinch-Leal closure approximation was adopted in the calculation of the constitutive equation set. The steady-state rheological behaviors predicted by adopting the Hinch-Leal approximation were compared with those by the Doi simple decoupling approximation. It could be predicted from the plot of N_1 versus $\bar{\tau}_{12}$ that smaller domains distributed isotropically at a quiescent state might maintain the isotropic domain distribution even at the imposition of moderate shear rate, and then could be changed to the ordered (or partially elongated) domain phase by a further increase of shear rate. Such change of the polydomain structure with the increase in shear rate could be proved more precisely by the transient rheological behaviors of N_1 and $\bar{\tau}_{12}$ after the start-up of shear flow.

Key words: *Liquid Crystalline Polymers, Polydomain Structure, Shear Flow, Rheological Behaviors*

INTRODUCTION

Liquid crystalline polymers (LCPs) usually show different rheological behaviors dominated by polydomain at low shear rates and monodomain at high shear rates. The theory of monodomain LCP rheology at high shear rates has been extensively appeared by Doi [1981], Kuzuu and Doi [1983, 1984], and See et al. [1990]. For the polydomain structure of LCPs at low shear rates, Marrucci [1985] first defined an effective domain size a and suggested a scaling law $a \propto (K/\eta\dot{\gamma})^{1/2}$ relating with shear rate $\dot{\gamma}$ where K is typical Frank elasticity constant and η (apparent viscosity. Many models [Larson and Mead, 1989; Marrucci and Maffettone, 1990a, b; Marrucci and Greco, 1992a, b] have been proposed to describe the polydomain or textured structure of LCPs and to correlate it with the rheological behaviors but they have provided just lumped features of polydomain LCPs.

Considering a LCP as a defect-laden polymeric fluid, Larson and Doi [1991] proposed a very promising theory for mesoscopic domains, which could provide a plausible description for the evolution of the defect density (or domain size) under shear flow. For steady rheological behavior, however, the defect density evolution equation can be applied only to the intermediate shear rate region (i.e., the well-known Onogi-Asada region II) but not to the low shear rate region (i.e., the Onogi-Asada region I) because it does not contain any intrinsic relaxation time in its steady-state scaling law. For the application to the low shear rate region, we have introduced the initial domain size a_o (or initial defect density L_o) to the Larson-Doi equation [Kim et al., 1994]:

$$\frac{dL}{dt} = \alpha\dot{\gamma}L - \beta\frac{K}{\eta}(L-L_o)^2 \text{ or } \frac{d(a^2)}{dt} = \beta\frac{K}{\eta}\left(1-\frac{a^2}{a_\delta^2}\right)^2 - \alpha\dot{\gamma}a^2 \quad (1)$$

Here, L denotes the defect density defined as a^{-2}. α and β are dimensionless constants keeping a typical rule of the Ericksen number $Er_{tex}=\beta/\alpha$-100 [Burghardt and Fuller, 1990] for shearing nematic LCPs. The idea of L_o or a_o was at first set to give a limit of domain coarsening after shear cessation, but Eq. (1) could be a possible one to cover the domain size evolution in shear rate region I as well as region II. With Eq. (1), the steady shear viscosity apparently showed the shear thinning behavior at low shear rates, reflecting the domain flow with a decrease in size or the effect of initial texture in the preparation [Kulichikhin, 1993].

Provided that smaller domains were distributed isotropically at the initial stage (not the equilibrium but just before the shear inception), another Newtonian plateau in the very low shear rate region, called "region 0", was also predicted and was recently observed by Sigillo and Grizzuti [1994] from nematic solutions of hydroxypropylcellulose in water. Comprehending some discussions given by Marrucci [1985, 1993, 1994] and Marrucci and Greco [1993], the Newtonian plateau and the shear thinning behaviors in regions 0 and I, respectively, might be due to the defect cores less ordered than nematic molecules or to a kind of domain isotropization process with the decrease in shear rate. The coupling of the defect cores and molecular disorder with the flow is expected to play a dominant role in controlling the rheological behavior of polydomain LCPs at low shear rates [Marrucci and Greco, 1993]. Based upon the evolution Eq. (1), thus, we will investigate the structural change of domains in the low shear rate region in an aspect of phenomenological steady shear property of LCPs. Transient shear and normal stresses after the abrupt imposition of low shear rate will be also examined to see how they approach to the steady-

†To whom all correspondences should be addressed.
*Current address: Department of Chemical Engineering, Pohang University of Science and Technology (POSTECH), P.O.Box 140, Pohang 790-600, Korea.

states and which factor of elastic and viscous properties more contributes to the steady-state shear flow.

CONSTITUTIVE EQUATION

We use a modified constitutive equation set of the domain-averaged Leslie-Ericksen theory or the Larson-Doi theory [1991] by including the idea of initial domain size [Kim et al., 1994]. The constitutive equation set used here, adopting the first closure approximation of Hinch-Leal (HL1) into both the stress expression and the order parameter evolution equation, can be referred to Kim and Chung [1996]. From the constitutive equation set, the steady-state shear stress ($\bar{\tau}_{12}$) and the first normal stress difference (N_1) can be calculated as functions of shear rate:

$$\bar{\tau}_{12}=\dot{\gamma}\left[\mu+\frac{2}{15}\mu_1+\frac{1}{3}\mu_2+\left(\frac{2}{5}\mu_1+\frac{1}{2}\mu_2\right)(\bar{S}_{11}+\bar{S}_{22})+\frac{4}{5}\mu_1\bar{S}_{12}^2+\frac{6}{5}\mu_1\bar{S}_{11}\bar{S}_{22}\right]-\frac{1}{2}(\alpha_3+\alpha_2)\varepsilon l_s\bar{S}_{12} \tag{2}$$

$$N_1=\left[2\mu_1\dot{\gamma}\bar{S}_{12}-\frac{1}{2}(\alpha_3+\alpha_2)\varepsilon l_s\right](\bar{S}_{11}-\bar{S}_{22}) \tag{3}$$

where $\bar{S}_{ij}$ is a mesoscopic order parameter tensor defined by $\bar{S}_{ij}=\langle[n_in_j]\rangle-\delta_{ij}/3$ for the director $\mathbf{n}$. The symbol $\langle[\cdots]\rangle$ means the average over mesoscopic domain space in the polydomain LCP system. Thus, the parameter tensor $\bar{S}_{ij}$ represents the second moment of domain orientation distribution, which allows the change in the average orientation state of domains but not the orientation at the molecular level. The steady-state shear component $\bar{S}_{12}$ can be obtained from a real root of the following equation

$$\lambda\dot{\gamma}^2\bar{S}_{12}\frac{5\varepsilon l_s+2\lambda(1-\lambda)\dot{\gamma}\bar{S}_{12}}{15(5\varepsilon l_s+2\lambda\dot{\gamma}\bar{S}_{12})^2}-\dot{\gamma}^2\bar{S}_{12}\frac{5\varepsilon l_s+4\lambda\dot{\gamma}\bar{S}_{12}}{5(\varepsilon l_s+2\lambda\dot{\gamma}\bar{S}_{12})^2}-\frac{4}{5}\lambda\dot{\gamma}\bar{S}_{12}^2+\frac{1}{5}\lambda\dot{\gamma}-\varepsilon l_s\bar{S}_{12}=0 \tag{4}$$

The approximate solution of $\bar{S}_{12}$ as a real root is calculated numerically by using a hybrid bisection-secant method, more precisely, the method of false position or *regula falsi* with setting the initial guess of $\bar{S}_{12}$ to zero and the tolerance value to 10^{-10}. Normal components of $\bar{S}_{ij}$ are

$$\bar{S}_{11}=\frac{\lambda\dot{\gamma}\bar{S}_{12}}{15\varepsilon l_s+6\lambda\dot{\gamma}\bar{S}_{12}}+\frac{\dot{\gamma}\bar{S}_{12}}{\varepsilon l_s+2\lambda\dot{\gamma}\bar{S}_{12}} \tag{5}$$

$$\bar{S}_{22}=\frac{\lambda\dot{\gamma}\bar{S}_{12}}{15\varepsilon l_s+6\lambda\dot{\gamma}\bar{S}_{12}}-\frac{\dot{\gamma}\bar{S}_{12}}{\varepsilon l_s+2\lambda\dot{\gamma}\bar{S}_{12}} \tag{6}$$

$$\bar{S}_{33}=\frac{\lambda\dot{\gamma}\bar{S}_{12}(4\lambda\dot{\gamma}\bar{S}_{12}-10\varepsilon l_s)}{75\varepsilon^2l_s^2-12\lambda^2\dot{\gamma}^2\bar{S}_{12}^2} \tag{7}$$

Other components of $\bar{S}_{ij}$, $\bar{S}_{13}$ and $\bar{S}_{23}$, may be set to zero from the value of the full refractive index tensor of $\langle[n_in_j]\rangle$ in sheared LCP solutions [Hongladarom and Burghardt, 1994]. In the calculations, we also use symmetrical, traceless properties of $\bar{S}_{ij}$. The steady-state defect annihilation rate l_s ($\equiv\beta KL_s/\eta$) is given by

$$l_s=l_o+\frac{\alpha\dot{\gamma}}{2}+\left[\alpha\dot{\gamma}\left(l_o+\frac{\alpha\dot{\gamma}}{4}\right)\right]^{1/2} \tag{8}$$

In the above equations, ε should be replaced by ε' [$\equiv\beta(\alpha_3-\alpha_2)\varepsilon/2\eta$] excluding the concentration dependence. Here, μ, μ_1, μ_2, and λ are constants determined by combinations of the Leslie viscosities α_i so that $\mu=\frac{\alpha_4}{2}$, $\mu_1=\frac{\alpha_1}{2}-\frac{(\alpha_2+\alpha_3)(\alpha_6-\alpha_5)}{2(\alpha_2-\alpha_3)}$, $\mu_2=\frac{\alpha_2\alpha_6-\alpha_3\alpha_5}{\alpha_2-\alpha_3}$, and $\lambda=\frac{\alpha_5-\alpha_6}{\alpha_3-\alpha_2}$. The values of α_i may be determined by Kuzuu-Doi theory [1983, 1984] for the given value of dimensionless molecular concentration C/C*. In lyotropic LCP system, higher values of C/C* than 1.122 means the nematic liquid crystalline phase. The possible range of L_o is 10^8-10^{10} m^{-2} corresponding to the initially coarsened texture length scale of 10-100 μm [Graziano and Mackley, 1984; Horio et al., 1985; Picken et al., 1991; Larson et al., 1992; Gleeson et al., 1992; Larson and Mead, 1992]. If typical values of parameters such as $K=10^{-11}$ N and $\eta=10$ Pa·s are chosen [Larson and Mead, 1992], the disclination annihilation rate l_o ($\equiv\beta KL_o/\eta$) of 0.001-0.1 s^{-1} corresponds to the range of L_o.

Transient shear properties can be also calculated by a numerical technique such as a multivariate Runge-Kutta method for the determinations of $\bar{S}_{ij}(t)$ and $l(t)$ as functions of time t after the abrupt imposition of shear rate. The transient shear stress $\bar{\tau}_{12}(t)$ [or $\bar{\tau}_{12}(\dot{\gamma}t)$] and the transient first normal stress difference $N_1(t)$ [or $N_1(\dot{\gamma}t)$] after the start-up are obtained by using $\bar{S}_{ij}(t)$ and $l(t)$ instead of $\bar{S}_{ij}$ and l_s, respectively, in Eqs. (2) and (3). As initial conditions for the transient calculation of the start-up process, we take $\bar{S}_{ij}(0)=0$ and $l(0)=l_o$ which are agreed with the initial state of polydomain LCPs [Kim and Chung, 1996].

STEADY RHEOLOGICAL BEHAVIORS

For our interest dealing with the rheological behaviors under weak shear flow, the shear rate region represented in the figures below excludes the region of shear thinning behavior (Onogi-Asada region III) under strong shear flow. Moreover, it should be emphasized that the steady-state rheological behaviors suggested in this paper are refreshed versions by adopting the HL1 concurrently to the stress expression and the order parameter evolution equation in order to be more appropriate for weak shear flow.

Fig. 1 shows the effects of initial domain size a_o (or the initial defect annihilation rate l_o) and molecular concentration C/C* on the steady-state domain anisotropy $\bar{S}_{11}-\bar{S}_{33}$, which means the degree of domain orientational order toward the flow direction. The trend of the increase in $\bar{S}_{11}-\bar{S}_{33}$ with shear rate is similar to that predicted by the modified Larson-Doi theory (see Fig. 7 of Kim et al. [1994]) which adopts the Doi simple decoupling approximation, but some aspects of the domain anisotropy are not. First, $\bar{S}_{11}-\bar{S}_{33}$ just reaches a value lower than 0.5 even when the shear rate increases up to 100 s^{-1} which is thought as the upper limit of region II, while the original Larson-Doi theory [1991] produces $\bar{S}_{11}-\bar{S}_{33}=0.781$ at C/C*=1.22 and $\varepsilon=0.03$ irrespective of shear rate. Experimentally, Hongladarom et al. [1993] showed that $\bar{S}_{11}-\bar{S}_{33}=0.53$-$0.63$ for 13.5 wt% and 20 wt% poly

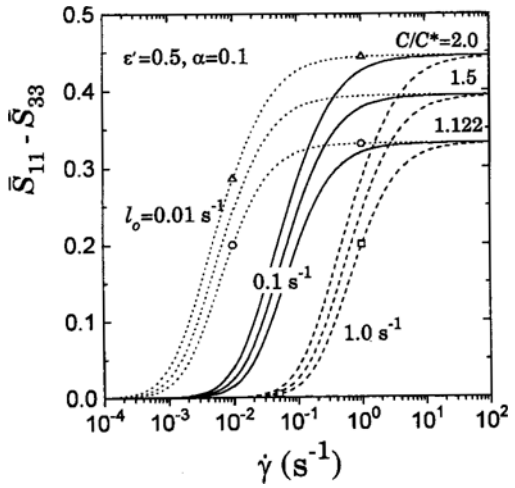

Fig. 1. Steady-state anisotropy ($\bar{S}_{11} - \bar{S}_{33}$) as functions of l_o and concentration parameter C/C*, which is calculated from the modified Larson-Doi constitutive equation set adopting the Hinch-Leal first approximation. Parameter values fixed in the calculation are ε'=0.5, η=10 Pa·s, K=10^{-11} N, α=0.1, and β=10. The symbols are for the discussion with Figs. 4 and 5.

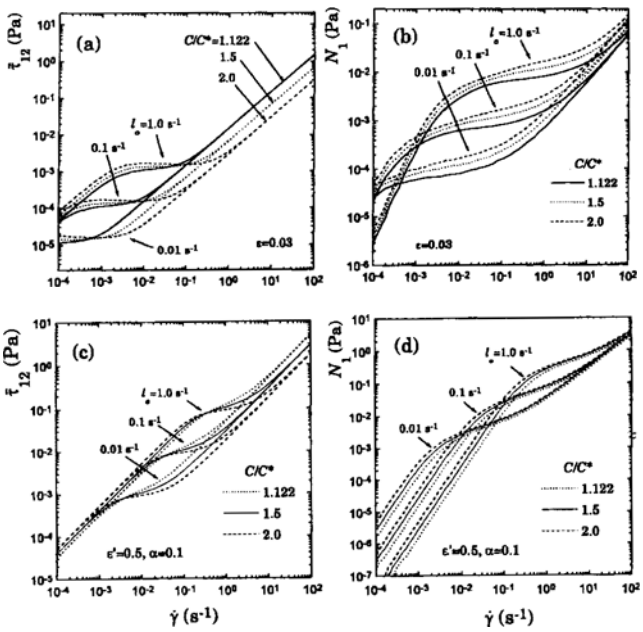

Fig. 2. (a), (c) Steady-state shear stress ($\bar{\tau}_{12}$) and (b), (d) first normal stress differences (N_1) calculated with increasing the shear rate ($\dot{\gamma}$), which are adopting (a), (b) the Doi simple decoupling approximation and (c), (d) the Hinch-Leal first closure approximation. Parameter values fixed in the calculation are ε'=0.5, η=10 Pa·s, K=10^{-11} N, α=0.1, and β=10.

(benzyl glutamate) solutions in *m*-cresol at the shear rate range of about 0.1-10 s^{-1}. These values of $\bar{S}_{11} - \bar{S}_{33}$ are better fitted with the present prediction than the case of adopting the Doi approximation. Second, the shear rate at which the abrupt increase of $\bar{S}_{11} - \bar{S}_{33}$ occurs is much increased when adopting the HL1. The difference is due to that the HL1 is most favorable to the weak shear flow, capable of allowing lower values of $\bar{S}_{11} - \bar{S}_{33}$ which result in not only in-plane but also out-of-plane domain alignments [Hongladarom and Burghardt, 1994] whereas the Doi decoupling approximation just means strong alignment of averaged domains (or monodomain state) under strong shear flow. From Fig. 1, thus, we may understand that the shear rate increases toward region II the domains become distributed to form a partially anisotropic phase corresponding to $\bar{S}_{11} - \bar{S}_{33}$= 0.550 between fully isotropic state ($\bar{S}_{11} - \bar{S}_{33}$=0) and perfect alignment of domains ($\bar{S}_{11} - \bar{S}_{33}$=1). The parameters l_o and C/C* show the same effects on $\bar{S}_{11} - \bar{S}_{33}$ as in the old version of Kim et al. [1994].

Steady-state shear stress $\bar{\tau}_{12}$ and first normal stress difference N_1 are shown in Fig. 2. The first two Figs. 2(a) and 2(b) are obtained by adopting the Doi simple decoupling while Figs. 2(c) and 2(d) by adopting the HL1. In Fig. 2(c), as the shear rate increases the shear stress $\bar{\tau}_{12}$, adopting HL1, gradually increases passing through a mound corresponding to the transition of steady shear viscosity from shear thinning (region I) to Newtonian plateau (region II) behaviors. The mound is just uplifted to the right hand when compared with Fig. 2(a) obtained from the Doi approximation. The adoption of HL1 also uplifts the N_1 behavior to the right hand. Then, the change in shear rate dependence of N_1 with increasing the shear rate, $N_1 \propto \dot{\gamma}^2$ to $\dot{\gamma}^1$, occurs at higher shear rate than the case of adopting Doi approximation. According to Kim et al. [1994], the change of $N_1 \propto \dot{\gamma}^2$ to $\dot{\gamma}^1$ corresponds to a transition from an isotropic domain phase into a more ordered domain phase with the increase in shear rate. The smaller domains are initially distributed (e.g., curves of l_o=1.0 s^{-1}), the higher shear rate is required to be the ordered or elongated domain phase. As a result, it can be said that the adoption of HL1 plays a role of protecting the less ordered domain phase to a certain extent from the external shear flow strength, as well as allows best fitting with the phenomenological transient shear stress after the start-up of shear flow [Kim and Chung, 1996].

In order to ascertain how the transition occurs during weak shear flow, we prepare a logarithmic plot of N_1 versus $\bar{\tau}_{12}$, as shown in Fig. 3, excluding the shear rate as a parameter. Such plot has been introduced by Han and Jhon [1986] with a concept that the two axes (the ordinate N_1 and the abscissa $\bar{\tau}_{12}$) ought to specify the elastic and viscous contributions, respectively, of the shearing polymeric liquids. Assuming the long-dashed straight line in Fig. 3 as a boundary on which the elastic and viscous contributions become equal (on the line the absolute values of N_1 and are $\bar{\tau}_{12}$ the same), the upper part of the line may be a region where the elastic contribution is dominant while the lower part corresponds to a dominant region of the viscous contribution.

As the shear rate increases, the curves in Fig. 3 linearly rise from the viscous region with the slope of 2, pass through a shoulder in the elastic region, and then constantly increase with the slope of 1 in the viscous region. The slopes of the curves directly corresponds to each domain phase with different distributions. The slope 2 at low shear rate indicates an isotropic distribution of domains. The isotropic distribution is preserved until the elastic energy density of the liquid crystalline molecules overrides the viscous energy density of shear flow strength.

Then, as the shear rate continually increases the isotropically distributed domains is gradually changed to a phase of ordered domains (or a partially elongated domain phase along the shear direction) producing the shoulder in Fig. 3. Knowing the shear rate at which the shoulder appears, the domain anisotropy corresponding to the shoulder can be checked out from Fig. 1 at the same shear rate. The domain anisotropy for the shoulder is proved to be the onset point of constant $\bar{S}_{11} - \bar{S}_{33}$ in Fig. 1 for each concentration. As the shear rate further increases (the curves proceed toward the upper part of Fig. 3), the domain anisotropy maintains unchanged, i.e., domain orientation does not change, but it seems that the domains are more elongated associating with the domain size reduction by the shear flow strength and tend to align with the shear direction, corresponding to the slope of 1 in the curves.

As shown in Fig. 3, the discussion in this stage may be divided into two cases, e.g., low and high concentrations. First, at low C/C* (e.g., curves of C/C*=1.122) small portion of anisotropic liquid crystalline phase is surrounded by high portion of isotropic defect phase (solvent molecules) in a lyotropic LCP solution. It seems that the domain elongation in this stage is due to the upsurge of external shear flow strength which is overriding the elasticity of liquid crystalline molecules. That is, higher portion of the defect phase is influenced more strongly by the shear flow rather than the anisotropic liquid crystalline molecules. Thus, the curve for the low C/C* under strong shear flow eventually arrives at the region of viscous contribution. In the case of high C/C* (e.g., curves of C/C*=2.0), the anisotropic domain phase share a greater portion than the isotropic defect phase, and thus the collective elastic property of liquid crystalline molecules within the domain can play a role of resisting the destruction of anisotropic domain phase, which may result in thinly elongated domains. Therefore, at this case of high C/C*, the curves rise monotonically in the region of elastic contribution. Of course, as the shear rate further increases up to the high shear rate in Onogi-Asada region III the viscous contribution eventually dominates the elastic contribution showing the shear thinning behavior, and the molecular-level dynamics of liquid crystal molecules [Doi, 1981; See et al., 1990] should start to be considered.

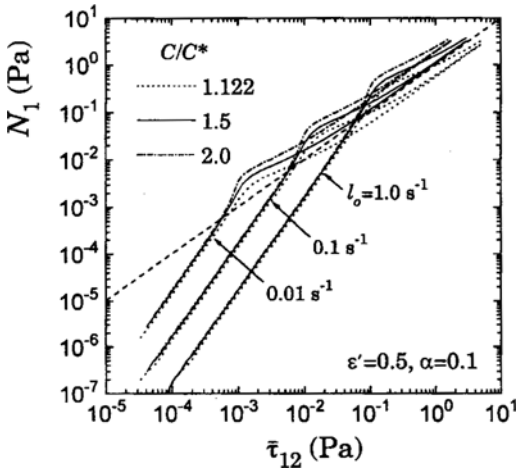

Fig. 3. Plot of N_1 versus $\bar{\tau}_{12}$ excluding $\dot{\gamma}$ as a parameter. The effect of shear rate is just potential along each curve. On the long-dashed straight line each value of N_1 and $\bar{\tau}_{12}$ becomes equal.

TRANSIENT RHEOLOGICAL BEHAVIORS AFTER THE START-UP

Transient shear stress $\bar{\tau}_{12}(\dot{\gamma}t)$ and transient first normal stress difference $N_1(\dot{\gamma}t)$ after the start-up of shear flow are appeared as damped oscillatory patterns against the total deformation or strain $\dot{\gamma}t$. According to many experimental results for the start-up [Metzner and Prilutski, 1986; Grizzuti et al., 1990; Kim and Han, 1993a,b], it is general that $N_1(\dot{\gamma}t)$ exhibits a higher amplitude and more fluctuated pattern than $\bar{\tau}_{12}(\dot{\gamma}t)$. This overwhelming effect of $N_1(\dot{\gamma}t)$ is also true for other transient shear flows such as step-up and flow reversal [Chow et al., 1992; Maffettone et al., 1994]. Rheological behaviors of $\bar{\tau}_{12}(\dot{\gamma}t)$ after the start-up was once discussed by Kim and Chung [1996]. Considering $\bar{\tau}_{12}(\dot{\gamma}t)$ associated with the behavior of N_1 $(\dot{\gamma}t)$, Fig. 4 is very useful to understand how the viscous and elastic energy densities contribute to the transient and even the steady-state shear behaviors along the shear rate. Such transient plot of $N_1(\dot{\gamma}t)$ versus $\bar{\tau}_{12}(\dot{\gamma}t)$ has been used [Maffettone et al., 1994; Moldenaers et al., 1994] to characterize the nonlinear dynamic features of LCP system. In the figures below, the absolute values of stresses are used and are not rescaled by their steady-state values in order to compare with the steady-state curves in Fig. 3.

Figs. 4 and 5 show the transient spirals prepared from $N_1(\dot{\gamma}t)$ and $\bar{\tau}_{12}(\dot{\gamma}t)$ after the start-up with the increase in shear rate. Associating with the damped oscillatory patterns of transient $N_1(\dot{\gamma}t)$ and $\bar{\tau}_{12}(\dot{\gamma}t)$, the spirals can be generally characterized by three features: the number of rotations (corresponding to the duration

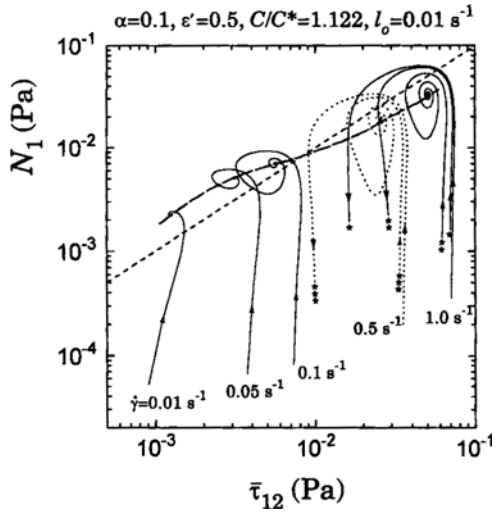

Fig. 4. Plot of transient N_1 versus $\bar{\tau}_{12}$ after the start-up of shear flow under the conditions of C/C*=1.122 and l_o=0.01 s^{-1}. Dotted straight line means the boundary on which the elastic contribution balances with the viscous contribution. Long-dashed curve is the locus of steady-states with increasing the shear rate in the start-up process. For the spirals of 0.5 and 1.0 s^{-1}, the same number of stars mean the connection via the negative values of N_1.

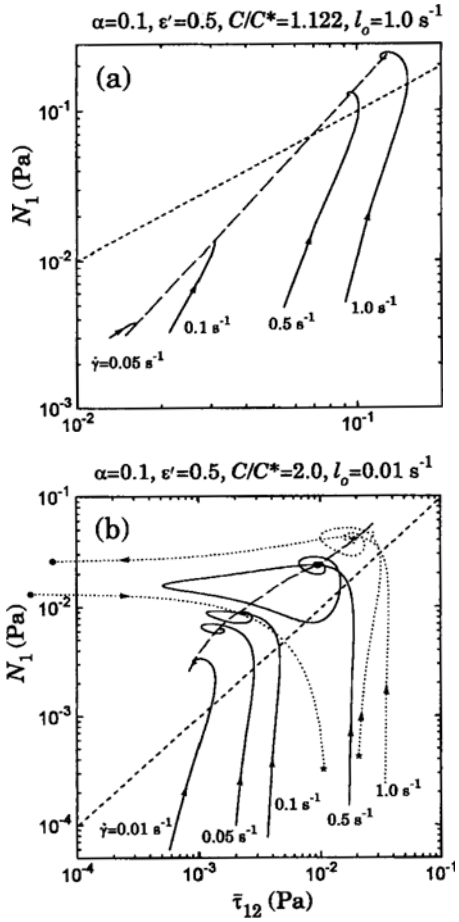

Fig. 5. Plot of transient N_1 versus $\bar{\tau}_{12}$ after the start-up of shear flow under the conditions of (a) C/C*=1.122 and l_o=1.0 s^{-1} and (b) C/C*=2.0 and l_o=0.01 s^{-1}. Other captions are referred to Fig. 4. For the spiral of 1.0 s^{-1}, solid circles mean the connection via the very low values of $\bar{\tau}_{12}$.

of oscillation peaks against total deformation), the maximum width of spiral (corresponding to the amplitude of the first overshoot), and the direction of spiral rotations. The counterclockwise direction of transient spirals is dominant in these figures except for the cases of very small domains initially distributed and of very low shear rates imposed [e.g., the slightly clockwise spiral for $\dot{\gamma}$=0.05 s^{-1} in Fig. 5(a)]. The dominance of the counterclockwise direction, meaning that the first maximum of $N_1(\dot{\gamma}t)$ appears at a higher strain value than that of $\bar{\tau}_{12}(\dot{\gamma}t)$, is consistent with the results from many transient processes [Metzner and Prilutski, 1986; Grizzuti et al., 1990; Chow et al., 1992; Kim and Han, 1993a,b; Maffettone et al., 1994; Moldenaers et al., 1994]. It is also understood as a factor belonging to the overwhelming effect of $N_1(\dot{\gamma}t)$ over the $\bar{\tau}_{12}(\dot{\gamma}t)$, which may be enhanced by the elastic property of the liquid crystal molecules.

As shown in Fig. 4, the number of rotations increases and the spirals become wider with increasing the shear rate, that is, the oscillations of $N_1(\dot{\gamma}t)$ and $\bar{\tau}_{12}(\dot{\gamma}t)$ grow in both intensity and duration. In the figure where the moderate parameter values of α=0.1, ε'=0.5, C/C*=1.122, and l_o=0.01 s^{-1} are given, the spiral at low shear rate travels from the viscous region to the elastic one and then terminates to their steady-state points in the elastic region. At high shear rates, the spirals cross over the viscous and elastic regions making some inner circles and proceed to the steady-state points in the viscous region. Though the quantitative changes of $N_1(\dot{\gamma}t)$ and $\bar{\tau}_{12}(\dot{\gamma}t)$ are not so large in the figure, it can be said that the resultant steady-state locus shows a transition of dominant contribution from the elastic to the viscous regions within the shear rate range of 0.01-1.0 s^{-1}. This corresponds to a curve portion between circles in Fig. 1 ($\bar{S}_{11}-\bar{S}_{33}$= 0.19-0.33) and depends on the change in the domain orientation and the domain size reduction (for size reduction, refer to Kim et al. [1994]).

Comparing Fig. 5 with Fig. 4, one may understand the effects of the initial domain size a_o (or the initial defect annihilation rate l_o) and concentration C/C* on the transient spirals. In Fig. 5(a), as a_o decreases (or l_o increases) the spirals rapidly terminate to their steady-state points with a few rotations, which corresponds to the domain anisotropy ($\bar{S}_{11}-\bar{S}_{33}$) within the range of 0.005-0.2 (the curve portion between rectangles in Fig. 1). Here, it should be noted that the initially isotropic phase of very small domains reaches its steady state with a slight fluctuation when even a moderate shear rate is imposed. Particularly, the spiral for a very low shear rate, such as 0.05 s^{-1} in Fig. 5(a), is slightly clockwise. The clockwise direction is caused from $N_1(\dot{\gamma}t)$ with just one peak and $\bar{\tau}_{12}(\dot{\gamma}t)$ without overshoot, which is a typical transient response of nearly isotropic domain phase ($\bar{S}_{11}-\bar{S}_{33}$=0.05 in this case). On the other hand, the steady-state locus linearly increases with a slope of 2 from the viscous region to the elastic region. It directly corresponds to the isotropic domain phase under weak shear flow in Fig. 3.

Comparing with Fig. 4, Fig. 5(b) is a version of increment in the concentration C/C* only. The increase in C/C* enhances the elastic contribution of liquid crystal molecules in a shearing nematic system. All spirals in Fig. 5(b) are counterclockwise and reflect severely fluctuating patterns of $N_1(\dot{\gamma}t)$ and $\bar{\tau}_{12}(\dot{\gamma}t)$ in the dominant region of elastic contribution. The domain anisotropy $\bar{S}_{11}-\bar{S}_{33}$ corresponding to the steady-state points of spirals are within 0.285-0.445 (see the curve portion between triangles in Fig. 1). This also means the establishment of domain alignment, which is similar to the case of Fig. 4 but different from that in the higher degree of domain alignment and in further increase of shear rate in the elastic region.

Comprehending the steady-state and transient rheological behaviors discussed above, we additionally suggest Fig. 6 which is the same figure as Fig. 1 but the boundaries on which the elastic contribution balances with the viscous contribution are included with respect to each initial domain size a_o or initial defect annihilation rate l_o. The boundaries shown as solid curves in Fig. 6 are obtained, on the basis of equal shear rate, by matching the value of $\bar{S}_{11}-\bar{S}_{33}$ in Fig. 1 with crossing point in Fig. 3 between the curves and the straight balance line. As a result, the upper part of each boundary is the dominant region of elastic contribution at fixed a_o or l_o, whereas the lower part the region of viscous contribution. It can be seen that as a_o decreases (or l_o increases) the boundary can shift to the high rate regions and may be extended to the lower $\bar{S}_{11}-\bar{S}_{33}$ region. This fact also supports that the smaller domains distributed isotropically can withstand the higher flow strength by the elasticity of liquid crystal molecules.

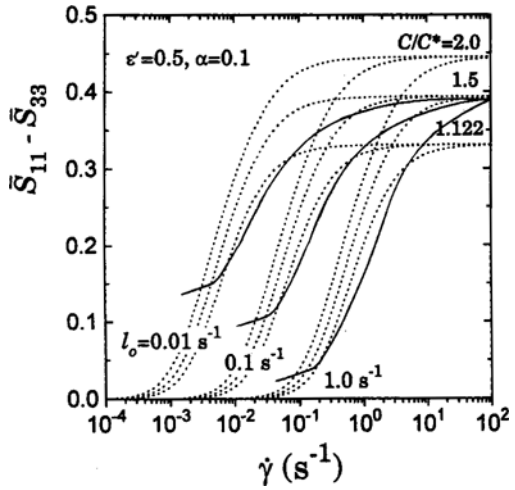

Fig. 6. Steady-state anisotropy ($\bar{S}_{11} - \bar{S}_{33}$) same as in Fig. 1 but the boundaries on which the elastic contribution balances with the viscous contribution are added with respect to each initial domain size a_o or initial defect annihilation rate l_o.

CONCLUDING REMARKS

We have investigated the structural change of a domain phase under weak shear flow, which has possibly occurred in shearing polydomain LCP. The phase transition from the isotropically distributed domains to the more ordered or elongated domains may be, to a certain extent, proved by the consideration of how elastic and viscous forces contribute to the shearing LCP system at low shear rates. However, there still remain some points to be studied: the lack of an accurate definition for the initial domain state, an imperfect description for the defect-core dynamics, at least a brief qualitative analysis for the elastic and viscous contributions, and so on. Despite such deficiencies, the present work will be helpful in understanding the importance of initial domain size in the LCP rheology at low shear rates.

As an additional feature to compact the theory one may consider the coupling the initial defect annihilation rate l_o with the shear rate $\dot{\gamma}$ to yield a dimensionless variable $l_o/\dot{\gamma}$ or $\dot{\gamma}/l_o$. This is due to the fact that the curves obtained at different l_o in the above figures can be superimposed by shifting the shear rate by exactly the same scale. The feature of superposition was mentioned previously in the domain shrinkage process after the shear inception [Kim et al., 1994], but associating with the defect core dynamics under shearing we have not obtained sufficient, exact data yet for the scaling relation between the two parameters. That is to say, for the simplification by examining the effect of the ratio $\dot{\gamma}/l_o$, it should be first known how fast the isotropic defect phase annihilates in all the steady-state, transient shear flows at a shear rate. The work on this topic is under consideration and the result will be presented.

ACKNOWLEDGEMENT

The authors (KMK and IJC) appreciate the Korea Research Foundation for the financial support under Non-Directed Research Fund (Grant No. 01-E-0543, 1994).

NOMENCLATURES

a : effective domain size
a_o : initial domain size
a_s : steady-state domain size
C/C*: dimensionless molecular concentration of liquid crystal molecules
Er_{tex} : texture Ericksen number ($\equiv\beta/\alpha$)
K : typical Frank elasticity constant
l : defect annihilation rate ($\equiv\beta KL/\eta$)
l_o : initial defect annihilation rate ($\equiv\beta KL_o/\eta$)
l_s : steady-state defect annihilation rate ($\equiv\beta KL_s/\eta$)
LCP : liquid crystalline polymer
L : defect density ($\equiv 1/a^2$)
L_o : initial defect density ($\equiv 1/a_o^2$)
L_s : steady-state defect density ($\equiv 1/a_s^2$)
n or n_i : director vector for an anisotropic domain
N_1 : steady-state first normal stress difference ($\equiv\bar{\tau}_{11} - \bar{\tau}_{22}$)
$N_1(\dot{\gamma}t)$: transient first normal stress difference [$\equiv\bar{\tau}_{11}(\dot{\gamma}t) - \bar{\tau}_{22}\ \dot{\gamma}t$]
$\bar{S}_{ij}$: mesoscopic order parameter tensor ($\equiv\langle[n_i n_j]\rangle - \delta_{ij}/3$)

Greek Letters

α_i : Leslie coefficients or Leslie viscosities (i=1-6)
α : a constant for viscous energy density ($\eta\dot{\gamma}$)
β : a constant for elastic energy density (K/a^2)
ε : an elasticity parameter
ε' : an elasticity parameter [$\equiv\beta(\alpha_3 - \alpha_2)\ \varepsilon/2\eta$]
$\dot{\gamma}$: shear rate
η : apparent viscosity
$\bar{\tau}_{12}$: steady-state shear stress
$\bar{\tau}_{12}(\dot{\gamma}t)$: transient shear stress

REFERENCES

Burghardt, W. R. and Fuller, G. G., "Transient Shear Flow of Nematic Liquid Crystals: Manifestations of Director Tumbling", *J. Rheol.*, **34**, 959 (1990).

Chow, A. W., Hamlin, R. D. and Ylitalo, C. M., "Transient Shear Response and Flow-Induced Microstructure of Isotropic and Nematic Rigid-Rod Poly(p-phenylenebenzothiazole) Solutions", *Macromolecules*, **25**, 7135 (1992).

Doi, M., "Molecular Dynamics and Rheological Properties of Concentrated Solutions of Rodlike Polymers in Isotropic and Nematic Liquid Crystalline Phases", *J. Polym. Sci., Polym. Phys. Ed.*, **19**, 229 (1981).

Gleeson, J. T., Larson, R. G., Mead, D. W., Kiss, G. and Cladis, P. E., "Image Analysis of Shear-Induced Textures in Liquid-Crystalline Polymers", *Liq. Cryst.*, **11**, 341 (1992).

Graziano, D. J. and Mackley, M. R., "Shear Induced Optical Textures and Their Relaxation Behaviour in Thermotropic Liquid Crystalline Polymers", *Mol. Cryst. Liq. Cryst.*, **106**, 73 (1984).

Grizzuti, N., Cavella, S. and Cicarelli, P., "Transient and Steady-State Rheology of a Liquid Crystalline Hydroxypropylcellulose Solution", *J. Rheol.*, **34**, 1293 (1990).

Han, C. D. and Jhon, M. S., "Correlation of the First Normal

Stress Difference with Shear Stress and of the Storage Modulus with Loss Modulus for Homopolymers", *J. Appl. Polym. Sci.*, **32**, 3809 (1986).

Hongladarom, K., Burghardt, W. R., Baek, S. -G., Cementwala, S. and Magda, J. J., "Molecular Alignment of Polymer Liquid Crystal in Shear Flows. 1. Spectrographic Birefringence Technique, Steady-State Orientation, and Normal Stress Behavior in Poly(benzyl glutamate) Solutions", *Macromolecules*, **26**, 772 (1993).

Hongladarom, K. and Burghardt, W. R., "Measurement of the Full Refractive Index Tensor in Sheared Liquid Crystalline Polymer Solutions", *Macromolecules*, **27**, 483 (1994).

Horio, M., Kamei, E. and Uchimura, H., "Dynamic Measurements on Polymer Liquid Crystals-Aqueous Solutions of Hydroxypropyl Cellulose", *Nihon Reoroji Gakkaishi*, **13**, 25 (1985).

Kim, K. M. and Chung, I. J., "Phenomenological Transient Shear Behavior of Liquid Crystalline Polymers after the Start-up of Shear Flow", *Macromol. Theory Simul.*, **5**, 145 (1996).

Kim, K. M., Cho, H. and Chung, I. J., "Defect Density Evolution and Steady Rheological Behaviors of Liquid-Crystalline Polymers", *J. Rheol.*, **38**, 1271 (1994).

Kim, S. S. and Han, C. D., "Effect of Molecular Weight on the Rheological Behavior of a Thermotropic Liquid-Crystalline Polymer", *Macromolecules*, **26**, 6633 (1993a).

Kim, S. S. and Han, C. D., "Transient Rheological Behavior of a Thermotropic Liquid-Crystalline Polymer. I. The Startup of Shear Flow", *J. Rheol.*, **37**, 847 (1993b).

Kulichikhin, V. G., "Rheological Properties of Liquid-Crystal Polymers", Liquid-Crystal Polymers, Platé, N. A., ed., Plenum Press, New York, 1993.

Kuzuu, N. and Doi, M., "Constitutive Equation for Nematic Liquid Crystals under Weak Velocity Gradient Derived from a Molecular Kinetic Equation", *J. Phys. Soc. Jpn.*, **52**, 3486 (1983).

Kuzuu, N. and Doi, M., "Constitutive Equation for Nematic Liquid Crystals under Weak Velocity Gradient Derived from a Molecular Kinetic Equation. II. Leslie Coefficients for Rodlike Polymers", *J. Phys. Soc. Jpn.*, **53**, 1031 (1984).

Larson, R. G. and Doi, M., "Mesoscopic Domain Theory for Textured Liquid Crystalline Polymers", *J. Rheol.*, **35**, 539 (1991).

Larson, R. G., Mead, D. W. and Gleeson, J. T., "Texture of a Liquid Crystalline Polymers during Shear", Proc. 11th Intern. Congr. Rheol., 65 (1992).

Larson, R. G. and Mead, D. W., "Development of Orientation and Texture during Shearing of Liquid-Crystalline Polymers", *Liq. Cryst.*, **12**, 751 (1992).

Larson, R. G. and Mead, D. W., "Time and Shear-Rate Scaling Laws for Liquid Crystal Polymers", *J. Rheol.*, **33**, 1251 (1989).

Maffettone, P. L., Marrucci, G., Mortier, M., Moldenaers, P. and Mewis, J., "Dynamic Characterization of Liquid Crystalline Polymers under Flow-Aligning Shear Conditions", *J. Chem. Phys.*, **100**, 7736 (1994).

Marrucci, G., "Rheology of Liquid Crystalline Polymers", *Pure Appl. Chem.*, **57**, 1545 (1985).

Marrucci, G., "Rheology of Thermotropic Liquid Crystalline Polymer", Thermotropic Liquid Crystalline Polymer Blends, La Mantia, F. P., ed., Technomic Pub., Lancaster, 1993.

Marrucci, G., "Non-linearity in Polymer Rheology", *J. Phys.: Condens. Matter*, **6**, A305 (1994).

Marrucci, G. and Greco, F., "A Molecular Approach to the Polydomain Structure of LCPs in Weak Shear Flow", *J. Non-Newtonian Fluid Mech.*, **44**, 1 (1992a).

Marrucci, G. and Greco, F., "The Polydomain Problem in Nematics. How to Account for Spatial Gradients in Molecular Orientation", Proc. 11th Intern. Congr. Rheol., 545 (1992b).

Marrucci, G. and Greco, F., "Flow Behavior of Liquid Crystalline Polymers", *Adv. Chem. Phys.*, **86**, 331 (1993).

Marrucci, G. and Maffettone, P. L., "Nematic Phase of Rodlike Polymers. I. Prediction of Transient Behavior at High Shear Rates", *J. Rheol.*, **34**, 1217 (1990a).

Marrucci, G. and Maffettone, P. L., "Nematic Phase of Rodlike Polymers. II. Polydomain Predictions in the Tumbling Regime", *J. Rheol.*, **34**, 1231 (1990b).

Metzner, A. B. and Prilutski, G. M., "Rheological Properties of Polymeric Liquid Crystals", *J. Rheol.*, **30**, 661 (1986).

Moldenaers, P., Mortier, M. and Mewis, J., "Transient Normal Stresses in Lyotropic Liquid Crystalline Polymers", *Chem. Eng. Sci.*, **49**, 699 (1994).

Picken, S. J., Aerts, J., Doppert, H. L., Reuvers, A. J. and Northolt, M. G., "Structure and Rheology of Aramid Solutions: Transient Rheological and Rheooptical Measurements", *Macromolecules*, **24**, 1366 (1991).

See, H., Doi, M. and Larson, R. G., "The Effect of Steady Flow Fields on the Isotropic-Nematic Phase Transition of Rigid Rod-like Polymers", *J. Chem. Phys.*, **92**, 792 (1990).

Sigillo, I. and Grizzuti, N., "The Effect of Molecular Weight on the Steady Shear Rheology of Lyotropic Solutions. A Phenomenological Study", *J. Rheol.*, **38**, 589 (1994).